

A Model of Mini-Embolic Stroke Offers Measurements of the Neurovascular Unit Response in the Living Mouse

Zheng Gang Zhang, MD, PhD; Li Zhang, MD; Guangliang Ding, PhD; Quan Jiang, PhD;
Rui Lan Zhang, MD; Xueguo Zhang, MD; Wen-Biao Gan, PhD; Michael Chopp, PhD

Background and Purpose—To measure cerebral vascular and neuronal responses after stroke in the living mouse, we generated a mouse model of embolic stroke localized to the parietal cortex.

Methods—Male C57/6J or male transgenic mice (2 to 3 months old) expressing yellow fluorescent protein (YFP) were used in the present study. A single fibrin-rich clot (8 mm in length) was injected into a branch of the right middle cerebral artery (MCA). MRI measurements were performed to measure ischemic lesion. Using confocal and 2-photon microscopy, changes in the embolus, dendrites, and dendritic spines were measured in the living mouse.

Results—Eight of 11 mice (73%) had the embolus localized to a branch of the right MCA in the parietal cortex. Expansion of the embolus within the artery was observed 24 hours after stroke. The presence of ischemic lesion in the parietal cortex was verified by MRI measurements, and histopathological analysis revealed that these mice (n=8) had a cortical infarct volume of $4.9 \pm 3.6\%$ of the contralateral hemisphere. In the living mouse, substantial loss of YFP-labeled axonal and dendritic structures as well as the formation of abnormal dendritic bulbs were detected in the ischemic boundary regions 24 hours after stroke compared with that 1 hour after stroke.

Conclusion—This model offers a novel approach to study the neurovascular unit in cerebral cortex after stroke in the living mouse. (*Stroke*. 2005;36:2701-2704.)

Key Words: cerebral ischemia ■ image ■ mice

Occlusion of a large cerebral artery results in acute cerebrovascular and parenchymal cellular dynamics as well as vascular and neural reorganization during the recovery period.¹⁻³ MRI measurements of these dynamic changes have provided much background information on focal cerebral ischemia and its neuropathologic consequences in the living animal.^{4,5} However, current understanding of changes of neuronal structures such as dendritic spines after stroke has been derived mainly from histopathology. Confocal and 2-photon laser scanning microscopy offers a noninvasive technique for evaluation of brain cellular dynamics with high resolution and has been used recently to measure dendritic spine stability in the adult cortex in the living transgenic mouse overexpressing yellow fluorescent protein (YFP) in pyramidal neurons.^{6,7} Measurements of dynamic neuronal alteration in response to stroke, particularly in genetically manipulated mice, would greatly enhance knowledge of pathophysiological consequences of stroke. Here, we describe a mouse model of embolic mini stroke in which a cortical branch of the middle cerebral artery (MCA) is occluded. Using this model and laser scanning confocal microscopy, we observed substantial changes in dendritic spines after stroke in the living mouse.

Materials and Methods

All experimental procedures have been approved by the institutional animal care and use committee of Henry Ford Hospital. Male C57/6J or male transgenic mice (2 to 3 months old) expressing YFP (H-line14)⁷ were purchased from The Jackson Laboratory (Bar Harbor, Maine).

Animal Model

Mice were anesthetized with 3.5% halothane and maintained with 1.0% halothane in 70% N₂O and 30% of O₂ using a face mask. Rectal temperature was maintained at 37°C throughout the surgical procedure by means of a feedback-regulated water heating system. Under the operating microscope (Carl Zeiss, Inc.) by a midline incision, the right common carotid artery, the right external carotid artery (ECA), and the right internal carotid artery (ICA) were isolated and carefully separated from the adjacent vagus nerve. A 6-0 silk suture was loosely tied at the origin of the ECA, and another suture was ligated at the distal end of the ECA. The right common carotid artery and ICA were temporarily clamped using a curved microvascular clip (Codman & Shurtleff, Inc.). The modified PE-50 catheter with a 0.15- to 0.18-mm OD containing a single intact fibrin-rich clot with a length of 8 mm was attached to a 100-L Hamilton syringe and was introduced into the ECA lumen through a small puncture. The suture around the origin of the ECA was tightened around the intraluminal catheter to prevent bleeding, and the microvascular clip was removed. A 9-mm-long catheter was gently advanced from the ECA

Received May 19, 2005; final revision received August 8, 2005; accepted September 23, 2005.

From the Department of Neurology (Z.G.Z., L.Z., G.D., Q.J., R.L.Z., X.Z., M.C.), Henry Ford Health Sciences Center, Detroit, Mich; Department of Physics (M.C.), Oakland University, Rochester, Mich; Molecular Neurobiology Program (W.-B.G.), Skirball Institute, and Department of Neuroscience and Physiology, New York University School of Medicine, New York.

Correspondence to Zheng Gang Zhang, MD, PhD, Department of Neurology, Henry Ford Hospital, 2799 W Grand Blvd, Detroit, MI 48202. E-mail zhazh@neuro.hfh.edu

©2005 American Heart Association, Inc.

Stroke is available at <http://www.strokeaha.org>

DOI: 10.1161/01.STR.0000190007.18897.e3

into the lumen of the ICA and reached the origin of the MCA. The clot was then gently injected with 100 μL of saline through the catheter. After injection of the embolus, the catheter was removed immediately. The present model of embolic stroke using an 8-mm-long clot is modified from that used previously (20-mm-long clot) to induce infarction encompassing the territory of the MCA.⁸ To identify localization of an embolus after injection, the fibrin-rich clot was labeled by Evans blue before injection. Briefly, the embolus was placed into 2% Evans blue solution (Sigma Chemicals) for 10 minutes and then washed twice with saline.⁹ To examine cerebral vessels, 100 μL of fluorescein isothiocyanate (FITC)-dextran (50 mg/mL; 2×10^6 molecular weight; Sigma) was injected intravenously after embolization.⁹

In Vivo Imaging

Methods for in vivo imaging have been described previously.⁶ Briefly, mice were anesthetized with an intraperitoneal injection (5.0 mL/kg) containing 17 mg/mL ketamine and 1.7 mg/mL xylazine in 0.9% NaCl. The skull was exposed and a region (≈ 1 mm in diameter) over the parietal cortex was located based on stereotactic coordinates. A high-speed drill (Fine Science Tools) was carefully used to reduce the skull thickness by $\approx 50\%$. To avoid damaging the underlying cortex by friction-induced heat, a cool sterile solution was added to the skull periodically, and drilling was intermittent to permit heat dissipation. Skull thinning was completed by gently scraping the cranial surface with a microsurgical blade. For optimal image quality, skull thickness was reduced to a very thin layer (≈ 20 μm). Using this method, we found that the majority of spines are stable over days to months in mice without MCA occlusion, indicating that this skull thinning technique does not cause changes in neuronal structures.^{6,10} To reduce respiration-induced movements, the skull was glued to a stainless steel plate 400-mm thick with a central opening for skull access. The plate was screwed to a homemade stereotaxic frame (Figure 1). After imaging, the plate was detached from the skull, the scalp was sutured, and the animal was returned to the cage until the next viewing.

For confocal microscopy imaging, the animal was inserted under a Nikon confocal microscope. A stack of image planes was acquired by using a water immersion objective lens ($\times 60$; 0.9 numerical aperture; Nikon). The imaging depth was ≈ 100 to 200 μm from the pial surface, and the step size was 0.70 μm . YFP was excited by a laser beam at 488 nm, and emissions were detected using a 522-nm emission filter.

For 2-photon microscopy imaging, the animal was inserted under a Bio-Rad Radiance 2-photon microscope (Bio-Rad).⁶ The Ti:sapphire laser was tuned to the excitation wavelength for YFP (920 nm) at a low laser power (< 40 mW at the sample) to minimize the possibility of phototoxicity. A stack of image planes was acquired by using a water immersion objective lens ($\times 60$; 0.9 numerical aperture; Olympus), an external detector, and a digital zoom of 3.0 to

4.0 \times . The imaging depth was ≈ 100 to 200 μm from the pial surface, and the step size was 0.70 μm . Two-dimensional projections of 3D image stacks containing dendritic segments of interest were used for all figures.

Using laser Doppler flowmetry (Perimed AB), regional cerebral blood flow (rCBF) was measured nearby (≈ 20 μm) the embolus, which we defined as the ischemic core, and the downstream area between the first and second branches of the occluded vessel, which is referred to as the penumbra.⁹

MRI Measurements

To confirm the ischemic lesion, diffusion-weighted MRI was performed on ischemic mice 1 hour after MCA occlusion using a 7.0-T magnet (Magnex Scientific) equipped with actively shielded gradients and an SMIS console.⁴

Measurements of Infarct Volume

At the end of experiments, animals were euthanized under anesthesia. Each mouse was transcardially perfused with heparinized saline followed by 10% formalin. The brain was removed from the skull and cut into 7 coronal blocks, each with 1-mm thickness. The brain tissue was processed, embedded, and 6- μm -thick paraffin sections from each block were cut and stained with hematoxylin and eosin for measurements of the ischemic lesion volume. The ischemic lesion volume was measured using a Global Laboratory Image analysis program (Data Translation). The ischemic volume is presented as the percentage of infarct volume of the contralateral hemisphere.^{8,11}

Results

A Single Clot Generates Parietal Cortical Infarction

Fluorescent microscopy and confocal microscopy showed that cerebral vessels perfused with FITC-dextran were readily visible through the thinned skull before injection of an embolus in the living mouse (Figure 2A). Immediately after injection of the embolus, the embolus was detected within a branch of the MCA in the parietal cortex (Figure 2B and 2C). rCBF in the ischemic core was reduced to 29 ± 3.2 and $31 \pm 2.2\%$ ($n=4$) of the contralateral levels 1 and 24 hours after embolization, respectively, whereas rCBF in the penumbra was 65 ± 9.2 (1 hour) and $75 \pm 13.9\%$ (24 hours) of the contralateral levels. Diffusion-weighted MRI measurements revealed an ischemic lesion localized in the parietal cortex 24 hours after the occlusion of the artery (Figure 2D). The parietal cortical lesion was confirmed by histology (Figure 2E). Quantitative analysis revealed that 73% of mice (8 of 11 mice) had the embolus localized to the right parietal cortical branch of the MCA and these mice had the cortical ischemic lesion volume of $4.9 \pm 3.6\%$ ($n=8$) of the contralateral hemisphere. In addition to the cortical lesion, 2 of 8 mice had the subcortical ischemic lesion infarct of $4.8 \pm 0.8\%$. However, we were not able to locate the clot in 3 of 11 mice and did not detect ischemic lesion in brains of these mice.

Parietal Cortical Stroke Induces Changes of Axons and Dendritic Spines

Using this model, we examined the effects of stroke on neuronal structures in living transgenic mice expressing YFP ($n=6$). One hour after occlusion of the parietal cortical branch of the MCA, YFP-labeled axons and dendrites were clearly visible in the region nearby the embolus in the parietal cortex (Figure 3A and 3B). High magnification revealed that structures of dendritic spines (Figure 3C) were comparable to

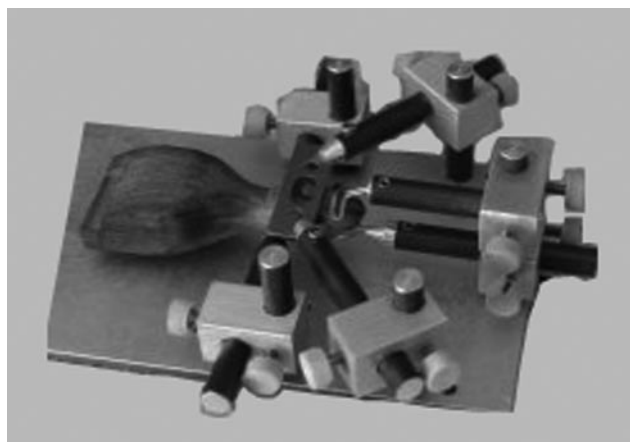


Figure 1. A homemade mini-stereotaxic frame.

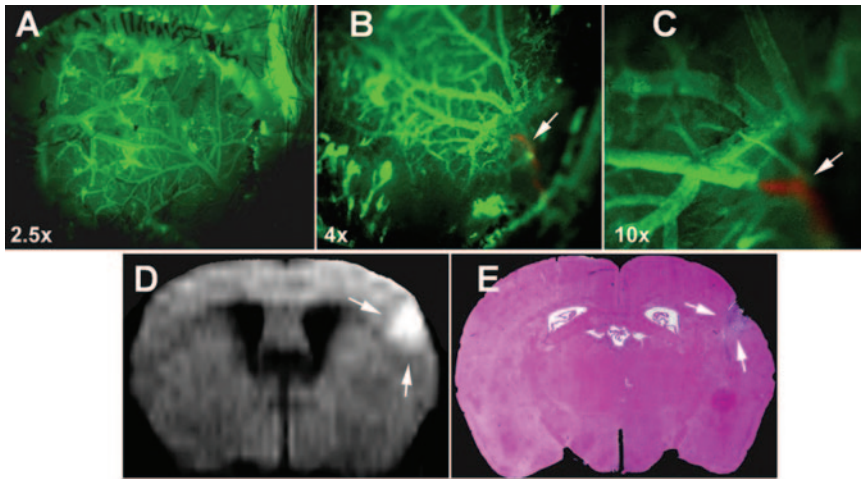


Figure 2. Generation of small cortical ischemia. A through C, Fluorescent microscopic images were acquired via a thin-skull window in the parietal cortex of the living mouse. Cerebral vessels perfused by FITC-dextran were clearly visible before injection of a clot (A). Injection of an Evans blue-labeled clot at origin of MCA blocked a branch of the MCA in the parietal cortex (B and C, arrows). D, Ischemic lesion in the parietal cortex was measured by diffusion-weighted MRI 24 hours after stroke. The parietal cortical lesion was confirmed by histology (E).

the structures of normal dendritic spines (Figure 3D). However, 24 hours after occlusion, the embolus expanded (Figure 3E, arrow) and endogenous thrombi were formed (Figure 3E, arrowhead). Numbers of YFP-labeled dendrites and axons were reduced substantially (Figure 3F). Dendritic bulbs and loss of spines were detected 24 hours after stroke (Figure 3G) compared with spines on dendrites at 1 hour after stroke (Figure 3C). The structures of dendritic spines obtained from the living mouse (Figure 3C and 3G) were comparable with that obtained from fixed brain tissue (Figure 3D). Loss of dendrites and spines as well as dendritic bulbs was confirmed when animals were euthanized (Figures 3H and 4A and 4B).

Discussion

In the present study, we describe a mouse model of mini-embolic stroke in the parietal cortex, and this model enables simultaneous monitoring of changes in embolus development and dendritic structures in response to stroke in the living mouse.

By ligating several cortical small arteries under open skull conditions, Wei et al generated a model of mini-stroke localized to the barrel cortex in the rat.¹² This model offers a

number of advantages, including *in vivo* measurements of angiogenesis development during the stroke repair period.^{12,13} However, excising the dura and manipulating cerebral arteries induce inflammatory reaction and formation of gliosis, which obscures the quality of *in vivo* microscopic measurements.¹³ We therefore thinned the skull, which preserves the natural status of the brain. The size of a clot determines infarct volume in models of embolic stroke.^{9,14} To occlude the origin of the MCA in the mouse, the length of a clot is ≈ 20 mm, which generates ischemic lesion that encompasses the entire territory supplied by the MCA.⁸ In the present study, we injected an 8-mm length of single fibrin rich clot into the intracranial segment of the ICA and found that 8 of 11 mice showed a clot lodged in the parietal cortical branch of the MCA, which resulted in the cortical infarction, suggesting that this model is reproducible. After injection of the clot, using microscopy, clot location and changes of the clot can be noninvasively monitored through the thinned skull. Thus, this model could be of benefit to many cerebral vascular pathological studies, including thrombosis, thrombolysis, and angiogenesis in living mice. Inability to detect a clot and the ischemic lesion in 3 of 11 mice suggests that a clot could be

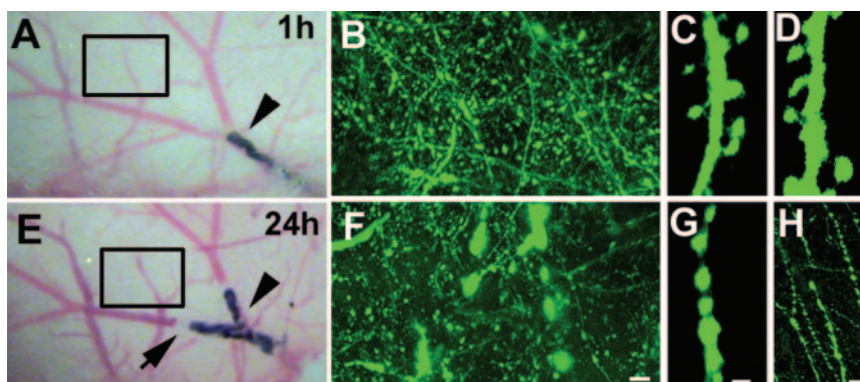


Figure 3. Transcranial 2-photon imaging in stroke brain of the living YFP mouse. A and E, Light microscopic views show that an Evans blue-stained clot (arrowheads) blocked a branch of the MCA in the parietal cortex below thinned skull 1 and 24 hours after stroke, respectively. B, C, F, and G, Two-dimensional projection of a 3D stack of dendritic branches and axons within the boxed area in A and E, respectively. The image depth was ≈ 100 μ m from the pial surface, and the step size was 0.7 μ m. D, Confocal image of spines on a dendrite of fixed brain tissue from a nonstroke mouse. Clot expanded at 24 hours (E, arrow), and numbers of dendrites and axons were reduced 24 hours (F) compared with 1 hour after stroke (B). High-magnification images show dendritic bulbs and loss of spines in living mouse (G) and fixed brain (H) 24 hours after stroke. Bars=5, 5, and 1 μ m in F, H, and G, respectively.

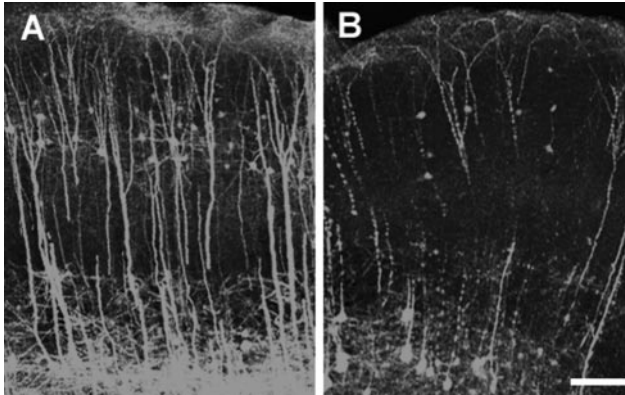


Figure 4. Single photon image of the cortex. A and B, Axons and dendrites in nonstroke and stroke cortex, respectively. Bar=100 μ m.

washed out the brain. In addition, 2 of 8 mice had subcortical ischemic lesion. Therefore, the model could be further improved.

Because of the large number and variability of neuronal connections, histopathological techniques do not provide accurate information on changes of neuronal structures over time.^{15,16} For example, by repeatedly imaging the same dendritic spines over months, we demonstrated previously that the majority of spines are stable in the cortex of adult mice,^{6,10} which has not been detected in histological studies. Using vascular morphology as a landmark, the present study demonstrated that dendritic structures in the penumbra did not change 1 hour after stroke. However, dendritic bulbs and loss of spines in this region were detected 24 hours after stroke, indicating that changes in axonal and dendritic structures in response to stroke could be dynamically measured in the living mouse using confocal or 2-photon microscopy without opening the skull. In parallel, using 2-photon microscopy, Zhang et al recently showed that moderate ischemia did not change dendritic structure within 5 hours, although severe ischemia caused loss of dendritic structures in 10 minutes.¹⁷ Thus, in addition to measuring dynamic changes in cerebral vessels, our model offers dynamical measurements of neuronal responses after stroke. Furthermore, stroke rats hosted in an enriched environment exhibit significant increases in spine density in the ischemic boundary region based on histopathological assessments,¹⁵ indicating that dendritic and spine plasticity is operating during stroke recovery. However, using 2-photon microscopy, we found recently that long-term sensory deprivation prevents net synapse loss in the living nonstroke adult mouse brain.¹⁸ Accordingly, it is important to dynamically monitor dendritic plasticity during stroke recovery in living animals, which could provide insights into mechanisms of brain plasticity. An additional potential ad-

vantage of this model is that the evolution of neurovascular responses to stroke could be monitored at the whole brain level by the MRI and at the cellular level by the confocal microscopy. In summary, the model of embolic stroke described here offers a novel approach to study neurovascular units in cerebral cortex after stroke in the living mouse.

Acknowledgments

This work was supported by National Institute of Neurological Disorders and Stroke grants PO1 NS23393, PO1 NS42345, RO1NS38292, and RO1HL 6476.

References

1. del Zoppo GJ. Microvascular changes during cerebral ischemia and reperfusion. *Cerebrovasc Brain Metab Rev*. 1994;6:47–96.
2. Lo EH, Broderick JP, Moskowitz MA. tPA and proteolysis in the neurovascular unit. *Stroke*. 2004;35:354–356.
3. Chopp M, Li Y. Treatment of neural injury with marrow stromal cells. *Lancet Neurol*. 2002;1:92–100.
4. Jiang Q, Zhang RL, Zhang ZG, Ewing JR, Divine GW, Chopp M. Diffusion-, t₂-, and perfusion-weighted nuclear magnetic resonance imaging of middle cerebral artery embolic stroke and recombinant tissue plasminogen activator intervention in the rat. *J Cereb Blood Flow Metab*. 1998;18:758–767.
5. Moonis M, Fisher M. Imaging of acute stroke. *Cerebrovasc Dis*. 2001;11:143–150.
6. Grutzendler J, Kasthuri N, Gan WB. Long-term dendritic spine stability in the adult cortex. *Nature*. 2002;420:812–816.
7. Feng G, Mellor RH, Bernstein M, Keller-Peck C, Nguyen QT, Wallace M, Nerbonne JM, Lichtman JW, Sanes JR. Imaging neuronal subsets in transgenic mice expressing multiple spectral variants of GFP. *Neuron*. 2000;28:41–51.
8. Zhang Z, Chopp M, Zhang RL, Goussev A. A mouse model of embolic focal cerebral ischemia. *J Cereb Blood Flow Metab*. 1997;17:1081–1088.
9. Zhang RL, Chopp M, Zhang ZG, Jiang Q, Ewing JR. A rat model of embolic focal cerebral ischemia. *Brain Res*. 1997;766:83–92.
10. Zuo Y, Lin A, Chang P, Gan WB. Development of long-term dendritic spine stability in diverse regions of cerebral cortex. *Neuron*. 2005;46:181–189.
11. Zhang L, Schallert T, Zhang ZG, Jiang Q, Arniago P, Li Q, Lu M, Chopp M. A test for detecting long-term sensorimotor dysfunction in the mouse after focal cerebral ischemia. *J Neurosci Methods*. 2002;117:207–214.
12. Wei L, Rovainen CM, Woolsey TA. Ministrokes in rat barrel cortex. *Stroke*. 1995;26:1459–1462.
13. Wei L, Erinjeri JP, Rovainen CM, Woolsey TA. Collateral growth and angiogenesis around cortical stroke. *Stroke*. 2001;32:2179–2184.
14. Overgaard K, Sereghy T, Boysen G, Pedersen H, Diemer NH. Reduction of infarct volume and mortality by thrombolysis in a rat embolic stroke model. *Stroke*. 1992;23:1167–1173.
15. Johansson BB, Belichenko PV. Neuronal plasticity and dendritic spines: Effect of environmental enrichment on intact and postischemic rat brain. *J Cereb Blood Flow Metab*. 2002;22:89–96.
16. Jones TA, Schallert T. Overgrowth and pruning of dendrites in adult rats recovering from neocortical damage. *Brain Res*. 1992;581:156–160.
17. Zhang S, Boyd J, Delaney K, Murphy TH. Rapid reversible changes in dendritic spine structure in vivo gated by the degree of ischemia. *J Neurosci*. 2005;25:5333–5338.
18. Zuo Y, Yang G, Kwon E, Gan WB. Long-term sensory deprivation prevents dendritic spine loss in primary somatosensory cortex. *Nature*. 2005;436:261–265.